IAC-19-B4,4,6,x51854

The ERNST mission: MWIR imaging and advanced technology demonstration in a 12 U nanosatellite

Clemens Horch[a]*, Martin Schimmerohn[a], Marius Bierdel[a], Stephan Busch[a], Max Gulde[a], Stefan Höffgen[b], Christoph Komrowski[bc], Stefan Metzger[b], Tobias Kündgen[b], Sven Ruge[b], Konstantin Schäfer[a], Michael Steffens[b], Caroline Schweitzer[d], Darren Sholes[a], Jonah Vincke[a], Erkai Watson[a], Frank Schäfer[a]

[a] *Fraunhofer Institute for High-Speed-Dynamics, Ernst-Mach-Institut, EMI, Ernst-Zermelo-Str. 4, 79104Freiburg, Germany*, clemens.horch@emi.fraunhofer.de
[b] *Fraunhofer Institute for Technological Trend Analysis INT, Appelsgarten 2, 53879 Euskirchen, Germany*
[c] *seneos GmbH, Josef-Lammerting-Allee 8, 50933 Köln, Germany*
[d] *Fraunhofer Institute of Optronics, System Technologies and Image Exploitation IOSB, Fraunhoferstr. 1, 76131Karlsruhe, Germany*
* Corresponding Author

Abstract

The ERNST (Experimental Spacecraft based on Nanosatellite Technology) mission is both a mid-wavelength infrared imaging satellite as well as a technology demonstrator. The 12 U nanosatellite is based on off-the-shelf CubeSat components where appropriate parts are available. All other subsystems and especially the main payloads are designed and built by Fraunhofer. The overall mission goal is to evaluate the utility of a large nanosatellite mission for scientific and military purposes.

ERNST's primary payload is a high-resolution mid-wavelength-infrared camera that is actively cooled by a Stirling cryo-cooler. This payload generates very demanding requirements for the satellite bus and exceeds the capabilities that are normally associated with CubeSats. This payload also demonstrates on-board data-processing using state-of-the-art FPGA technology and comprises a filter pendulum mechanism for switching between several spectral bands. The payload data is transmitted to the ground segment in X-Band. All components of this payload are mounted on an optical bench which has been designed using numerical topology optimization methods and is 3D-printed from an aluminum alloy. Integrated into this optical bench is a 3D-structured radiator that dissipates the heat generated by the cryo-cooler.

The second payload is a radiation sensor by Fraunhofer INT that characterizes the radiation environment in ERNST's orbit by measuring electrons and protons from the radiation belts and from solar storms. The radiation sensing is based solely on counting the number of changed bits in memory devices behind different shielding thicknesses to distinguish between different types of particles and energies. Furthermore, ERNST hosts an optical camera payload in the visual spectrum.

The ERNST 12U platform provides flexible payload capabilities with high-data rate processing and download, as well as 60 W beginning-of-life power provided by two deployable solar arrays. The most complex mechanism on board is a drag-sail subsystem to de-orbit the ERNST nanosatellite after its mission end for ensuring the sustainability of space applications.

Keywords: CubeSat, infrared, radiation, additive manufacturing, de-orbit

Acronyms/Abbreviations

Advanced Encryption Standard (AES)
Attitude Determination and Control System (ADCS)
Computer Aided Design (CAD)
Consultative Committee for Space Data Systems (CCSDS)
Central Processing Unit (CPU)
Data Processing Unit (DPU)
Electrical Power Subsystem (EPS)
Erasable Programmable Read-Only Memory (EPROM)
Experimental Spacecraft based on Nanosatellite Technology (ERNST)
Engineering Qualification Model (EQM)
Field Programmable Gate Array (FPGA)
Galois Counter Mode (GCM)
Indium antimonide (InSb)
Mid-Wavelength Infrared (MWIR)
On-Board-Computer (OBC)
Printed Circuit Board (PCB)
Solar Energetic Particle (SEP)
Single Event Upset (SEU)
Selective Laser Melting (SLM)
System-on-Chip (SoC)
System-on-Module (SoM)
Static Random-Access Memory (SRAM)
Telemetry and Telecommand (TCTM)
Total Ionizing Dose (TID)

1. Introduction

ERNST is a 12U nanosatellite hosting a mid-wavelength infrared (MWIR) imager as its main payload. ERNST is short for Experimental Spacecraft based on

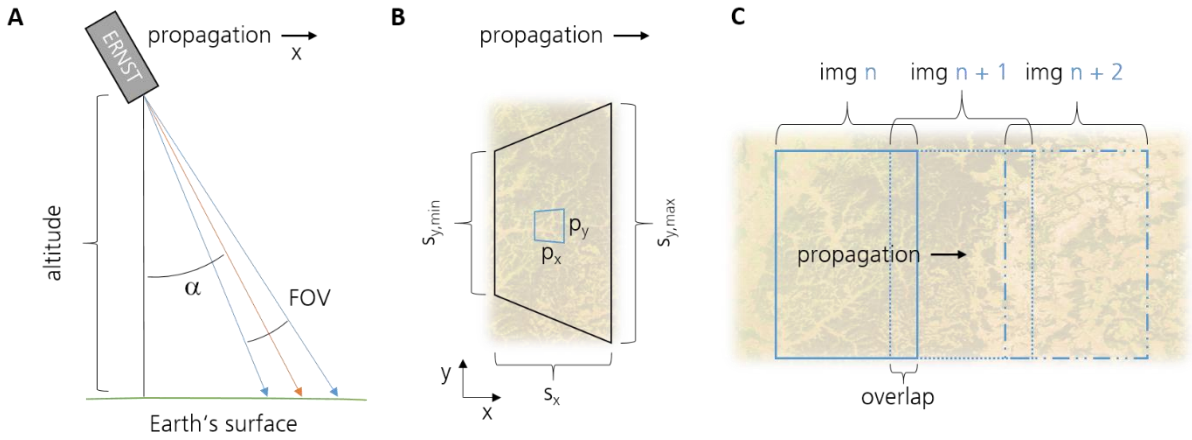

Fig. 1: ERNST pointing and image recording. A: Satellite pointing forward by α with respect to nadir. B: Exaggerated perspective distortion of the recorded image with indicated swath width S_y. Pixel footprint $p_x \times p_y$. C: Contiguity of images per band ensured by overlap of sequentially recorded images.

Nanosatellite Technology and its primary goal is to evaluate the utility of a nanosatellite mission for scientific and military purposes. Besides the infrared imager, the satellite carries a camera in the visual spectrum and a radiation monitoring payload. Furthermore, the satellite is used as a technology demonstration platform. Most notably, a deployable de-orbit drag-sail and additive manufacturing technology will be demonstrated in space.

The underlying idea of ERNST is the evaluation of the utility of a 12U nanosatellite platform. This size class can be seen as a compromise between the usually smaller CubeSats and the larger microsatellites of the 100kg class. The 12U size combines advantages of both: from the CubeSats it inherits the large choice of affordable components and the containerized launch. At the same time, it removes many constraints of the smaller systems. A 12U platform allows for much more relaxed power and mass budgets and most importantly provides enough space for larger optics.

The challenges and opportunities that arise from integrating a 12U satellite from CubeSat components have been discussed in more detail in [1] and [2]. The tailored thermal design methodology that has been developed specifically for the ERNST mission is presented by Gulde et al. [3–5]. [6] describes the ERNST mission with a special focus on the infrared payload. Even more details on the payload and its data processing system can be found in [7]. Schweitzer et al. [8] describe the detection and tracking of launch vehicles as an application for the infrared imaging payload in ERNST. Schimmerohn and Bierdel et al. [9–11] provide more details on the additive design and manufacturing methodology that ERNST demonstrates. The development of its de-orbit drag-sail has been presented by Sinn et al. [12] and Reichenbach et al. [13].

This paper gives an overview and update on the ERNST mission and spacecraft design. It describes the main payloads as well as the technology demonstrated.

2. The ERNST Mission

The ERNST mission is designed around the main payload. While the launcher and therefore the final orbit is not yet determined, we aim for a 500-600km sun-synchronous orbit.

The MWIR imager is designed to accomplish two objectives: the search and tracking of ballistic missiles during their boost phase [8] as well as the continuous observation of the earth's surface in two spectral bands. At an altitude of 700 km, the detector has a swath width of 164 km, resulting in a pixel footprint of up to 112 x 145 m². The optics are optimized for a large swath width rather than the highest ground resolution. For the continuous recording of the Earth's surface, the pointing of the satellite is 30° with respect to nadir in the direction of travel (Fig. 1A). At an altitude of 700 km, the detector has in a swath width of 164 km (Fig. 1B), resulting in a pixel footprint of maximally 112 x 145 m^2.

In this mode, the payload's spectral filters are iterated at a frequency of 0.1 Hz, which allows for the recording of continuous, connected stripes in each band with an image-to-image overlap of about 10 % (Fig. 1C).

In a second mode, ERNST observes a specific region of interest as long as possible. In this scenario, the satellite slowly rotates in order to fix the intersection of the detector's optical axis with Earth's surface for as long as possible. The resulting maximum angular speed is 0.6°s^{-1}.

The minimal size of the monitored area is around 10.000 km^2, represented by a rectangle with dimensions of 115 km x 92 km.

3. The ERNST Satellite Platform

One purpose of the ERNST project is the evaluation of the utility of a 12U platform in comparison with both smaller CubeSats and larger microsatellites. The question is whether it is possible to integrate a sophisticated payload that would usually require a larger platform into a satellite that is built, where possible, from existing CubeSat subsystems. In order to answer this question, solutions currently market have been evaluated and suitable components were chosen which fulfill the requirements. Where suitable components are not available, in-house solutions have been developed. In particular, ERNST uses an OBC, EPS, UHF transceiver (COM) and a camera in the visual spectrum from GomSpace [14], an X-Band transmitter and antenna from Syrlinks [15] and an integrated ADCS. The satellite structure, the solar generators, the payload DPU as well as the de-orbit drag-sail and the radiation monitoring payload have been developed by Fraunhofer. A rendered view of the ERNST CAD model is shown in Fig. 2.

Fig. 2: CAD-Model of the ERNST satellite. The 3D-printed parts are highlighted with orange color.

The power subsystem is designed for a beginning-of-life power generation of 60W. Up to 20W of this power is used in the MWIR payload, particularly by the detector's cryo-cooler. Consequently, the thermal design is a key part of the satellite design. Mission analysis identified the need for a dedicated thermal radiator which has been designed using numerical optimization methods and manufactured from an aluminum alloy using the SLM process at Fraunhofer EMI.

The electrical subsystem makes use of the CubeSat de-facto standard PC/104 [16] for the interconnection of subsystems. In order to overcome incompatibilities between subsystems from different venders a backplane design [1] has been implemented with in total four different PC/104 stacks.

The TCTM communcation is performed in the UHF band. ERNST is equipped with a deployable UHF antenna. The payload data is transmitted in the X-Band using a patch antenna with 8dBi gain. The X-Band link is compliant to a CCSDS protocol stack [17–19] and is capable of encrypting the data stream in real-time using the CCSDS Space Data Link Security Protocol [20] and AES-GCM encryption [21].

In the ground segment, Fraunhofer EMI operates its own ground station for TCTM. The payload data downlink is performed via a commercial ground station network.

4. Technology Demonstration

4.1. Additive Design and Manufacturing

A central part of ERNST's technology demonstration is the additively manufactured optical bench and thermal radiator as shown in Fig. 3. This structural element is being manufactured by Fraunhofer EMI using the well-established SLM process using a high-quality industrial system (EOS M 400). It is able to process structures with maximum $400 \times 400 \times 400$ mm^3 volume and provides 1000 Watts laser power.

Fig. 3: Additively manufactured payload support structure and radiator.

The optical bench has been designed using a finite-element numerical approach for optimizing the topology with respect to the loads and boundary conditions [10]. The goal is a lightweight structure that is robust against deformations under vibrational loading and ensures a fast and homogeneous temperature transfer.

Fig. 4 shows the overall design process. First, we defined the payload components to be mounted on the optical bench and the mechanical loads acting on the system during rocket launch (plus qualification margins) and the thermal loads occurring during operation in orbit. Then, we identify the design space, i.e. the volume that is available for placing structures after removing non-design areas that are needed to accommodate other components or to allow access to it.

We combine standard acceleration and vibration loads and define a stiffness goal with the first eigenfrequency >100 Hz. The solution of the

optimization task has a bionic appearance with relatively high geometric complexity. We simplify the geometry and include functional design elements for mounting (for components and for post-processing) in a hybrid CAD approach [22]. This combination of non-parametric and parametric CAD concepts enables easy design changes in the optimized structure. Finally, we verify the adequacy of the final design of the optical bench by numerical frequency response and thermal analysis. The maximum root mean square von-Mises stress response found is four orders of magnitude lower than the yield strength of the aluminum alloy.

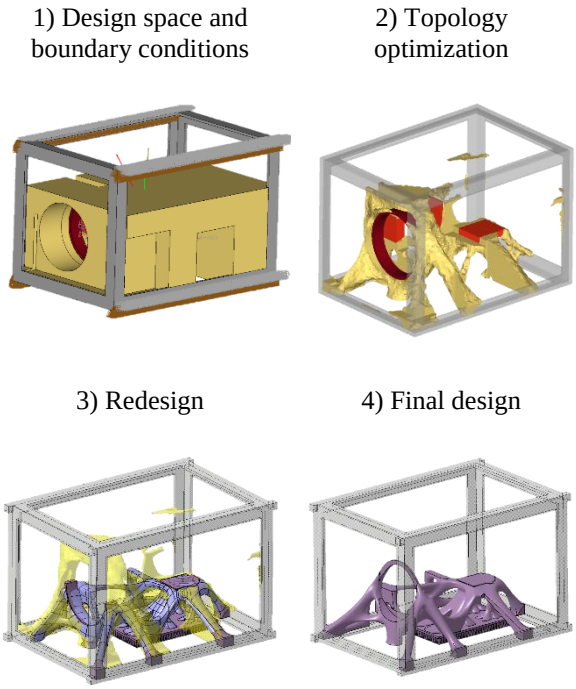

Fig. 4: Design process for additive manufacturing

4.2. De-Orbit Sail

In order to fulfil the space debris mitigation guidelines, ERNST is equipped with a de-orbit drag-sail. The entire subsystem fits into a 1U CubeSat footprint and is scalable for satellites weighing up to 50 kg. For its first mission, a drag-sail surface area of 2.5 m² is chosen which provides sufficient projected area for ERNST.

Particular focus was placed on designing a de-orbit system that it is applicable for non-operational, tumbling spacecraft. A watchdog timer (with sufficient timeout and redundant design) triggers the deployment of the drag-sail. Only the electric energy for actuating a hold-down-release-mechanism is needed to start the deployment of the drag-sail.

The mechanical deployment involves a two-step process. A telescoping mechanism simultaneously drives the stored deployable structure out of its 1U housing while releasing the sail deployment. The deployable structure is composed of robust tape spring booms, rolled into an unstable configuration onto one central boom spool, eliminating the need for additional power springs or motors to drive the deployment. After investigating different sail folding options, we use a four-piece sail that is stowed in individual cartridges to enable controlled deployment and procurable membrane material.

The engineering qualification model has been integrated and is currently undergoing comprehensive functional and environmental testing to verify the robustness against cold welding and other long-term storage effects. A proto-flight model based on our design was launched on Rocket Lab's Electron kick-stage last December. We hope for another demonstration of our de-orbit subsystem before its first operation as part of the ERNST mission in 2021.

5. Payloads

ERNST hosts three payloads. The main payload is the MWIR imager which defines most mission parameters. In addition, there is a commercially available camera in the visual spectrum. Finally, ERNST carries a scientific radiation monitoring device.

5.1. MWIR Imaging Payload

The mid-wavelength infrared imager (see Fig. 5) consists of a commercially available infrared optics, a filter pendulum for switching between multiple spectral bands and the infrared detector unit. The detector unit comprises a 1.3 Megapixel InSb sensor with a spectral range of 3-5 µm. The detector is actively cooled by a cryo-cooler. This cooler posed one of the biggest challenges during the payload design, as it generates substantial heat and vibrations. All optical components are mounted to the optical bench described in section 4.1, page 3.

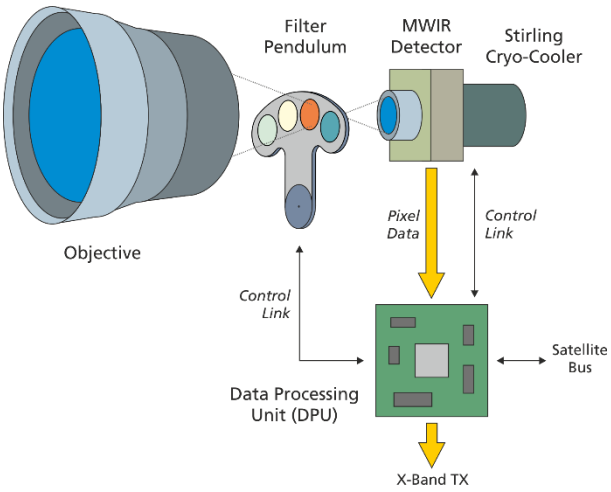

Fig. 5: MWIR imaging payload block diagram

The detector unit provides the image data via a serial high-speed interface to the DPU, which handles the processing and storage of the captured image data as well as the controlling of the payload's subsystems. The DPU can be seen as a successor to the DPU currently flying on the Kent Ridge 1 microsatellite [23] and will also be on-board of NExSat [24]. The DPU's hardware is based on a SoC combining an FPGA and a powerful CPU. The DPU hardware design is based on SoM-approach. The SoM daughterboard sits on top of the main DPU circuit board and complements the main SoC with all required peripherals like DDR RAM, flash memory and power supply circuits on a small PCB. Besides the simplification of the hardware development, this concept allows us to switch between different FPGA SoCs with no or minimal changes to the custom baseboard. Currently, we are using an SoC from the Zynq-7000 Series by Xilinx [25]. With the SoM concept, we can switch to the newer Zynq UltraScale+ MPSoC [26] for later versions of the DPU without having to design a new FPGA board.

The programmable logic part of the FPGA SoC fulfills multiple tasks. The first is to provide all non-standard hardware interfaces to the CPU. We use custom IP cores to implement the performance sensitive interfaces to the MWIR detector and the X-Band transmitter. Secondly, the FPGA implements computationally intensive algorithms to reduce the CPU load.

The DPU's software is based on a custom-tailored embedded Linux operating system. The DPU performs all image processing that is required for infrared imaging. This includes everything from bad pixel replacement and non-uniformity correction to lossless image compression using the JPEG2000 [27] or FELICS [28, 29] algorithms. Furthermore, the software is responsible for managing the acquired data in the various storage media. Finally, the DPU software controls the detector and the filter pendulum and is able to provide a CCSDS conforming data stream for downlink.

More details on the MWIR imaging payload can be found in [7] and [30].

5.2. Radiation Detector Payload

Ionizing radiation is the most severe environmental factor impacting electronics in space. Despite this significance most satellites fly without any kind of radiation sensor to measure the actual radiation levels of the electronics inside the satellite. Such a sensor would be extremely useful to:

- compare the dose predicted and qualified on the ground with the actually received dose,
- autonomously detect solar particle events,
- enable adaptive radiation mitigation techniques and
- support anomaly investigation.

In order to increase the acceptance of satellite manufacturers, the radiation sensor should be simple, robust, cheap and easy to integrate. Since even small CubeSat satellites contain today a significant quantity of microcontrollers, we propose to exclusively use memory chips as radiation detectors, namely SRAMs and EPROMs.

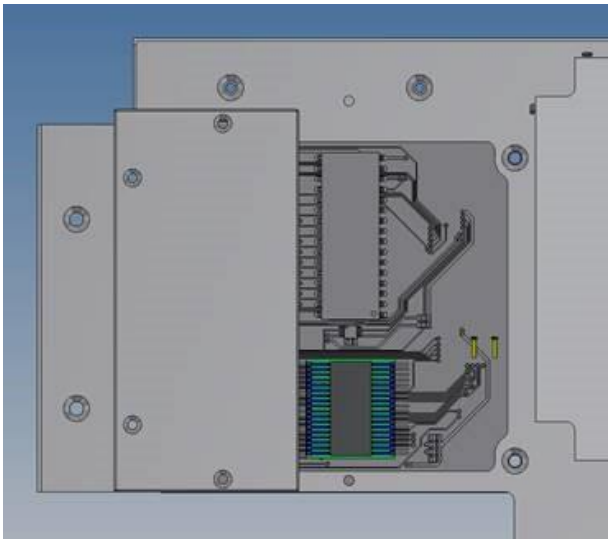

Fig. 6: View on the Sensor board of the radiation detector, containing two SRAMs and two EPROMs, one part of each is located behind a defined additional aluminium shield.

SRAMs are made from a series of bistable latching circuits that store the information. Densely ionizing radiation, either directly as cosmic rays or SEPs or indirectly as secondary particle from reactions with protons, can change the state of the information (SEU). If the sensitivity of the SRAM is known, in our case on ERNST the AT60142H 4Mbit SRAM from Atmel, then the number of upsets per time gives a direct measurement of the flux of the densely ionizing particles. The AT60142H 4Mbit is used for the ESA SEU monitor and therefore its sensitivity to all kinds of radiation is very well known [31].

EPROMs store the information in transistors having a floating gate. During the programming the floating gate is populated with electrons whose charge change the threshold voltage of the transistor. Ionizing radiation depopulates the floating gate, eventually putting the transistor back in its unprogrammed state. Thus, the number of the deprogrammed bits is a direct measurement of the received TID of the chip. For the radiation detector on ERNST a UV-EPROM (M27C801 100FG from STMicroelectronics) is used. With the UV light it is possible to depopulate the floating gates gradually up to the point where some start to change their digital state. Prepared in such a way, it is possible to

immediately measure the effects of the ionizing radiation [32].

Both sensors are also built into the Fraunhofer module on board the Heinrich Hertz satellite (H2SAT) [33] described in [34]. Since ERNST will fly in a LEO orbit with a much more benign radiation environment compared to the geostationary orbit of the H2SAT, the memory chips are put on a board facing directly to the outside, getting them in direct contact with the radiation environment. The board as shown in Fig. 6 contains two chips of each type. One chip of each type is placed behind a shield with defined thickness. This allows for the SRAM to discriminate the particles into two energy bins and for the EPROM to distinguish between TID produced by both electrons and protons and TID produced only by protons, by shielding the less penetrating electrons.

6. Qualification

The ERNST EQM is currently undergoing the necessary qualification tests at Fraunhofer EMI. This especially includes thermal-vacuum and vibration testing. All tests having been performed until today on a component or subsystem-level have been successful. The system level test is scheduled for late 2019. Therefore, results cannot be presented in this paper.

Shortly after the qualification tests we will start building the ERNST flight model. The launch is currently scheduled for the second half of 2021.

7. Conclusions

In this paper we presented the 12 U nanosatellite ERNST. It hosts three payloads and multiple technology demonstrators. The main payload is an advanced, cryo-cooled mid-wavelength infrared imager with FPGA-based data-processing. The idea behind ERNST is to provide an agile and modular satellite bus that uses the advances of the CubeSat market dynamics with sophisticated standardized bus components while providing sufficient space and power for more complex instruments through its 12U format. After its launch, ERNST will demonstrate the capabilities of this 12U platform in orbit. We focus on military as well as scientific applications. In addition, we think much of ERNST's design and technology can be applied to next generation earth observation missions.

8. References

[1] C. Horch, M. Schimmerohn, and F. Schäfer, "Integrating a large nanosatellite from CubeSat components – Challenges and solutions," in *68th International Astronautical Congress (IAC)*, Adelaide, Australia, 2017.

[2] F. Nohka, M. Drobczyk, and A. Heidecker, "Experiences in Combining Cubesat Hardware and Commercial Components from Different Manufacturers in order to build the Nano Satellite AISat/Clavis-1," in *26th Annual AIAA/USU Conference on Small Satellites*, Logan, USA, 2012.

[3] M. Gulde, J. Montemayor Mancías, C. d. Genova, M. Schimmerohn, and F. Schäfer, "Reliable, fast, and flexible: A thermal modeling approach for small satellites," in *32nd Annual AIAA/USU Small Satellite Conference 2018. Online resource*, 2018, p. 5.

[4] M. Gulde, J. Montemayor Mancías, M. Schimmerohn, and F. Schäfer, "Fast view factor determination for thermal modelling," in *European Space Thermal Engineering Workshop 2018. Proceedings*, 2018, pp. 297–312.

[5] M. Gulde *et al.*, "Managing high thermal loads in small satellites - analysis, design, and verification of a 3D-printed radiator," in *68th International Astronautical Congress (IAC)*, Adelaide, Australia, 2017.

[6] C. Horch, M. Schimmerohn, M. Gulde, and F. Schäfer, "ERNST: A 12U Infrared Imaging Nanosatellite based on CubeSat Technology," in *4S Symposium 2018*, Sorrento, Italy, 2018.

[7] C. Horch *et al.*, "An MWIR payload with FPGA-based data processing for a 12U nanosatellite," in *Small Satellites for Earth Observation. 11. International Symposium of the International Academy of Astronautics 2017*, 2017, pp. 339–342.

[8] C. Schweitzer *et al.*, "Nanosat-based detection and tracking of launch vehicles," in *8th International Symposium on Optronics in Defence & Security*, Paris, France, 2018.

[9] M. Schimmerohn *et al.*, "Additive manufactured structures for the 12U nanosatellite ERNST," in *32nd Annual AIAA/USU Small Satellite Conference 2018. Online resource*, 2018, p. 5.

[10] M. Bierdel, A. Pfaff, M. Jäcklein, M. Schimmerohn, and M. Wickert, "Multidisciplinary Design Optimization of a Satellite Structure by Additive Manufacturing," in *68th International Astronautical Congress (IAC)*, Adelaide, Australia, 2017.

[11] M. Bierdel, K. Hoschke, A. Pfaff, M. Schimmerohn, and F. Schäfer, "Towards flight qualification of an additively manufactured nanosatellite component: Paper presented at 69th International Astronautical Congress, Bremen, Germany, October 1-5, 2018," in *69th International Astronautical Congress (IAC)*, Bremen, Germany, 2018, p. 6.

[12] T. Sinn *et al.*, "The development of a passive de-orbit subsystem for small and micro satellites," in *68th International Astronautical Congress (IAC)*, Adelaide, Australia, 2017.

[13] N. Reichenbach, T. Sinn, M. Schimmerohn, and M. Langer, "Lessons Learnt on the Development of a De-Orbit Subsystem for the 12U-CubeSat ERNST," in *Advanced Lightweight Structures and Reflector Antennas: Proceedings of the 3rd International Conference*, Tblisi, Georgia, 2018.
[14] *GomSpace*. [Online] Available: https://gomspace.com/.
[15] J.-L. Issler *et al.*, "CCSDS communication products in S and X band for CubeSats," in *28th Annual AIAA/USU Conference on Small Satellites*, Logan, USA, 2014.
[16] PC/104 Embedded Consortium, "PC/104 Specification: Version 2.6," Oct. 2008.
[17] Consultative Committee for Space Data Systems, "TM Synchronization and Channel Coding," Recommended Standard 131.0-B-2, Aug. 2011.
[18] Consultative Committee for Space Data Systems, "AOS Space Data Link Protocol," Recommended Standard 732.0-B-2, Jul. 2006.
[19] Consultative Committee for Space Data Systems, "Encapsulation Service," Recommended Standard 133.1-B-2, Oct. 2009.
[20] Consultative Committee for Space Data Systems, "Space Data Link Security Protocol," Recommended Standard CCSDS 355.0-B-1, Sep. 2015.
[21] Consultative Committee for Space Data Systems, "CCSDS Cryptographic Algorithms," Recommended Standard CCSDS 352.0-B-1, Nov. 2012.
[22] K. Hoschke, M. Bierdel, and M. Wickert, "Topology and Shape Optimization with Hybrid CAD design for Additive Manufacturing," *NAFEMS Benchmark*, Jul. 2017.
[23] T. Segert *et al.*, "Kent Ridge 1 - a hyper spectral micro satellite to aid disaster relieve," in *AIAA/USU Conference on Small Satellites*, 2014.
[24] T. Segert and N. P. Nagendra, "The 3 Levels of Small Satellite Capacity Building. Explained with Real World Examples.," in *67th International Astronautical Congress (IAC)*, Guadalajara, Mexico, 2016.
[25] Xilinx Inc., Ed., "Zynq-7000 All Programmable SoC Overview," DS190, Sep. 2016.
[26] Xilinx Inc., Ed., "Zynq UltraScale+ MPSoC Data Sheet: Overview," DS891, Feb. 2017.
[27] ITU-T, *Recommendation T.800: JPEG 2000 image coding system: Core coding system*.
[28] P. G. Howard and J. S. Vitter, "Fast and Efficient Lossless Image Compression," in *DCC `93: Data Compression Conference*, Snowbird, Utah, USA, 1993, pp. 351–360.
[29] A. G. Bhosale and P. S. Bidkar, "A Modified Image Template for FELICS Algorithm for Lossless Image Compression," *International Journal of Current Engineering and Technology*, vol. 4, no. 3, pp. 1785–1789, Jun. 2014.
[30] C. Horch, N. Domse, F. Schäfer, and M. Buhl, "High level software development for a stand-alone data processing and storage unit for a microsatellite hyperspectral payload," in *Small satellites for earth observation. Digest of the 10th International Symposium of the International Academy of Astronautics (IAA) 2015*, 2015, pp. 207–210.
[31] R. Harboe-Sorensen *et al.*, "From the Reference SEU Monitor to the Technology Demonstration Module On-Board PROBA-II," *IEEE Transactions on Nuclear Science*, vol. 55, no. 6, pp. 3082–3087, 2008.
[32] L. Z. Scheick, P. J. McNulty, and D. R. Roth, "Dosimetry based on the erasure of floating gates in the natural radiation environments in space," *IEEE Transactions on Nuclear Science*, vol. 45, no. 6, pp. 2681–2688, 1998.
[33] A. Hofmann, R. Wansch, R. Glein, and B. Kollmannthaler, "An FPGA based on-board processor platform for space application," in *2012 NASA/ESA Conference on Adaptive Hardware and Systems (AHS)*, 2012, pp. 17–22.
[34] S. Metzger *et al.*, "Fraunhofer satellite radiation sensing systems," *Acta Astronautica*, vol. 162, 2019.